International Journal of Latest Engineering and Management Research (IJLEMR)
ISSN: 2455-4847
www.ijlemr.com || REETA-2K16 ǁ PP. 117-127

Minimization of AC and DC Faults in VSC-HVDC Transmission System using FLC

Uppara Hari Shankar[1], S.Rakesh[2] & T.Madhuranthaka[3]
[1]*P.G. Scholar, Department of EEE, S.V. College of Engineering, Tirupati, A.P., INDIA*
[2]*Asst.Professor, Department of EEE, S.V. College of Engineering, Tirupati, A.P., INDIA*
[3]*HOD, Department of EEE, S.V. College of Engineering, Tirupati, A.P., INDIA*

Abstract: This paper proposes a new technique for minimization of ac and dc faults in voltage source control HVDC transmission system using Fuzzy Logic Controller (FLC). The proposed HVDC transmission system offers current limiting capability during dc-side fault. This feature eliminates the need of dc-side circuit breakers in dc power transmission system and filter design by generating higher pulse level. Additionally, it offers features such as smaller footprint and a larger active and reactive power capability curve than existing VSC-based HVDC systems, including those using modular multilevel converters. To illustrate the feasibility of the proposed HVDC system, this paper assesses its dynamic performance during steady-state and network alterations, including its response to ac and dc side faults.

Keywords: DC fault reverse blocking capability, hybrid multilevel converter with ac side cascaded H-bride cells, modular multilevel converter, voltage-source-converter high-voltage dc (VSC-HVDC) transmission system, fuzzy logic controller (FLC).

I. INTRODUCTION

With increased demand for clean energy, power system networks need to be reengineered to be more efficient, flexible and reinforced to accommodate increased penetration of renewable power without compromising system operation and reliability. A VSC-HVDC transmission system is a candidate to meet these challenges due to its operational flexibility. With the continued increase of power and voltage levels, stress on cost effective solutions and stringent guidelines for power quality, multilevel converters have emerged as a technically viable solution for accomplishing acceptable standards. The term 'Multilevel' has been coined to emphasize the ability to increase the instantaneous voltage levels in steps, accomplished by addition of components in series. The basic topologies are Diode Clamped, Flying Capacitor, Cascaded H-bridge and the Modular Topology. Although the different topologies offer a variety of advantages, they however, also possess some limitations with further increase in voltage levels. In the last decade, voltage-source-converter high-voltage dc (VSC-HVDC) transmission systems have evolved from simple two-level converters to neutral-point clamped converters and then to true multilevel converters such as modular converters [1]–[5].

The VSC-HVDC system offers the operational flexibility, such as provision of voltage support to ac networks, its ability to operate independent of ac network strength therefore makes it suitable for connection of weak ac networks such as offshore wind farms, suitability for multi-terminal HVDC network realization as active power reversal is achieved without dc link voltage polarity change, and resiliency to ac side faults (no risk of commutation failure as with line-commutating HVDC systems)[6]–[12]. However, vulnerability to dc side faults and absence of reliable dc circuit breakers capable of operating at high-voltage restrict their application to point-to-point connection.

Present VSC-HVDC transmission systems rely on their converter station control systems and effective impedance between the point-of-common-coupling (PCC) and the converter terminals to ride-through dc side faults. With present converter technology, the dc fault current comprises the ac networks contribution through converter free-wheeling diodes and discharge currents of the dc side capacitors (dc link and cable distributed capacitors) [13], [14]. The magnitude of the dc-side capacitors' discharge current decays with time and is larger than the ac networks contribution. For this reason, dc fault interruption may require dc circuit breakers that can tolerate high let-through current that may flow in the dc side during the first few cycles after the fault, with high current breaking capacity and fast interruption time. Recent HVDC converter topologies with no common dc link capacitors, such as the modular multilevel converter (M2C), may minimize the magnitude and duration of the discharge current first peak. [2], [13], [15].

This paper presents a new HVDC transmission systems based on a hybrid-voltage-source multilevel converter with ac-side cascaded H-bridge cells. The adopted converter has inherent dc fault reverse-blocking capability, which can be exploited to improve VSC-HVDC resiliency to dc side faults. With coordination

between the HVDC converter station control functions, the dc fault reverse-blocking capability of the hybrid converter is exploited to achieve the following:

- During dc fault, eliminate the ac grid contribution with dc system, hence minimizing the risk of converter failure due to uncontrolled over current.
- Due to a reduction in the magnitude and duration of the dc fault current, simplify dc circuit breaker design.
- Improve voltage stability of the ac networks as converter reactive power consumption is reduced during dc-side faults.
- Facilitate controlled recovery without interruption of the VSC-HVDC system from dc-side faults without the need for opening ac-side circuit breakers;

The rest of this paper is organized as follows. The operational principle and control of the hybrid voltage source multilevel converter with ac-side cascaded H-bridge cells topology is briefly described in Section II. The Fuzzy logic controller and the HVDC system control design, detailed block diagram that summarizes how different control layers of the proposed HVDC transmission system are interfacing with FLC is discussed in Section III. Simulation results are presented in Section IV to demonstrate its response during network disturbances. Included are simulations of ac and dc fault ride-through capabilities. Finally, the conclusions are given in Section V.

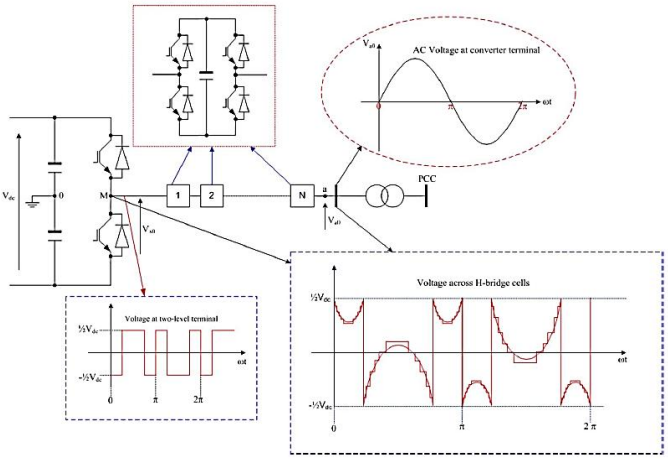

Fig. 1. Hybrid voltage multilevel converter with ac side cascaded H-bridge cells.

II. HYBRID MULTILEVEL VSC WITH AC-SIDE CASCADED H-BRIDGE CELLS

Fig. 1 shows one phase of a hybrid multilevel VSC with H-bridge cells per phase. It can generate voltage levels at converter terminal "a" relative to supply midpoint "0." Therefore, with a large number of cells per phase, the converter presents near pure sinusoidal voltage to the converter transformer as depicted in Fig. 1 [1]. The two-level converter that blocks high-voltage controls the fundamental voltage using selective harmonic elimination (SHE) with one notch per quarter cycle, as shown in Fig. 1. Therefore, the two-level converter devices operate with 150-Hz switching losses, hence low switching losses and audible noise are expected. The H-bridge cells between "M" and "a" are operated as a series active power filter to attenuate the voltage harmonics produced by the two-level converter bridge. These H-bridge cells are controlled using level-shifted carrier-based multilevel pulse width modulation with a 1-kHz switching frequency. To minimize the conversion losses in the H-bridge cells, the number of cells is reduced such that the voltage across the H-bridge floating capacitors sum to (1/2) Vdc. This may result in a small converter station, because the number of H-bridge cells required per converter with the proposed HVDC system is one quarter of those required for a system based on the modular multilevel converter. With a large number of cells per phase, the voltage waveform generated across the H-bridge cells is as shown in Fig. 1, and an effective switching frequency per device of less than 150 Hz is possible.

The dc fault reverse-blocking capability of the proposed HVDC system is achieved by inhibiting the gate signals to the converter switches, therefore no direct path exists between the ac and dc side through freewheel diodes, and cell capacitor voltages will oppose any current flow from one side to another. Consequently, with no current flows, there is no active and reactive power exchange between ac and dc side during dc-side faults. This dc fault aspect means transformer coupled H-bridges cannot be used. The ac grid contribution to dc-side fault current is eliminated, reducing the risk of converter failure due to increased current stresses in the switching devices during dc-side faults. From the grid standpoint, the dc fault reverse-blocking

capability of the proposed HVDC system may improve ac network voltage stability, as the reactive power demand at converter stations during dc-side faults is significantly reduced. The ac networks see the nodes where the converter stations are connected as open circuit nodes during the entire dc fault period. However, operation of the hybrid multilevel VSC requires a voltage-balancing scheme that ensures that the voltages across the H-bridge cells are maintained at Vdc/N under all operating conditions, where Vdc is the total dc link voltage. The H-bridge cells voltage balancing scheme is realized by rotating the H-bridge cell capacitors, taking into account the voltage magnitude of each cell capacitor and phase current polarity. An additional PI regulator is used to ensure that the cell capacitors be maintained at Vdc/N as depicted in Fig. 4.

III. FUZZY LOGIC CONTROLLER

Fuzzy logic becomes more popular due to dealing with problems that have uncertainty, vagueness, parameter variation and especially where system model is complex or not accurately defined in mathematical terms for the designed control action. The conception of the fuzzy logic introduced by Zadeh [16] is a combination of fuzzy set theory and fuzzy inference system (FIS). Elements of a fuzzy set belong to it with a certain degree, called degree of membership. The degree of membership is a result of mapping the input to certain rules using a membership function (MF). The progression which maps the specified input data to the output using fuzzy logic is known as fuzzy inference.

A fuzzy inference system can be classified as:

a) Fuzzification: which is the process of converting any crisp value to analogous linguistic variable based on certain MF,
b) Knowledge base: consists MF definitions and necessary rules like IF-THEN or it is combination of condition part with their associated rules
c) Inference engine: simulates human decision,
d) Defuzzification: is the progression of transforming the fuzzy output into a crisp numerical value.

In this paper main control input variable is the DC-link voltage error and output of FLC is the peak value of the reference source current. The range of operating current, normalization and de-normalization is one of the important design factors of fuzzy controller. The block diagram representation of fuzzy logic controller with inference system is shown in Fig. 2. The scaling factor Ge, Gce, and Gu are used to scaling the input and outputs as per the designing of FLC.

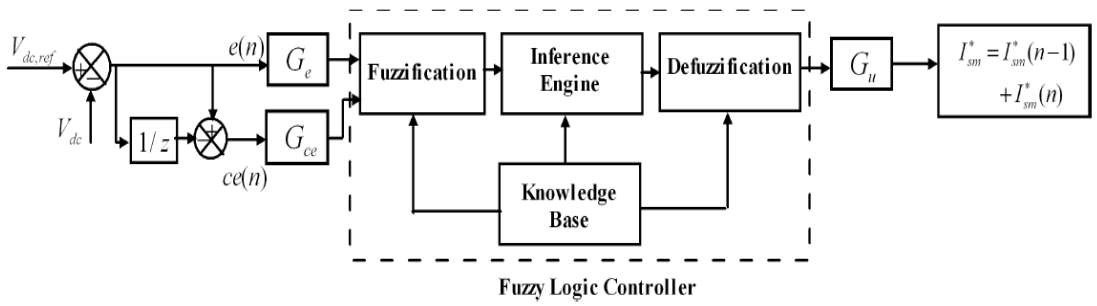

Fig. 2. Detailed structure of fuzzy logic controller

A. Designing of control rules:

Computational methods determine the computational efficiency, processor memory requirement and processing time. The fuzzy control rules based on membership function defining or relate input variables to output variables. The number and type of MF determines the computational efficiency of fuzzy control technique. The determination of MFs depends on the designer's experience and knowledge. The shape decision of MFs affects how well a fuzzy system rules approximate a function. Triangles or triangular membership function (TMF) have been frequently used in several applications of FLC [22], [23]. TMF are preferred due to simplicity, easy implementation, symmetrical along the axis. Fig. 3 shows the MFs relating input and output linguistic variables. The number of linguistic variables is directly related to the accuracy of approximating function and plays an important role for input-output mapping [24]. However, some limits have to consider while designing number of linguistic variables in view of accuracy and complexity of FLC.

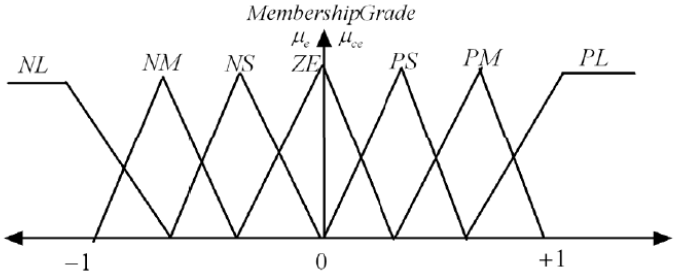

Fig. 3(a) Error 'e' and change in error 'ce'

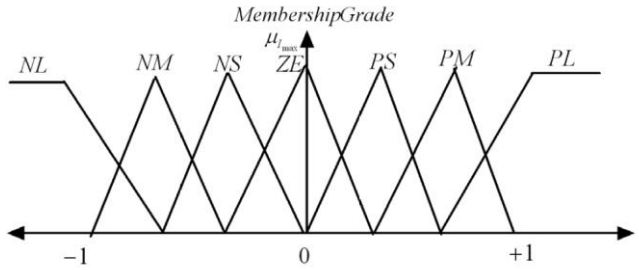

Fig. 3(b) Change in reference output current
Fig. 3. Triangular shaped membership function used in fuzzification

The error e and change of error ce at nth sampling instant are used as input of FLC and can be written as [17]:

$$e = Vdc,ref - Vdc$$

$$ce(n) = e(n) - e(n-1)$$

The output of FLC with limiter is considered as amplitude of derived reference current (I*sm). In this paper seven triangular membership functions have been chosen for representing numerical variables into linguistic variables [18], viz., NL (negative large), NM (negative medium), NS (negative small), ZE (zero), PS (positive small), PM (positive medium), PL (positive large). The spacing between MFs may be equal or unequal; it is set here for cover a band of load current with good accuracy. After this rules formation as knowledge base, different inference mechanisms have been developed for defuzzify fuzzy rules. In this paper, authors apply Mamdani's max-min inference method to get an implied fuzzy set of tuning rules. Finally center of mass method is used defuzzify the implied control variables.

The above can be summarized as for implementing FLC:

1) First, scaling factors consist of the normalization gain for input and de-normalization gain is selected properly.
2) Rules decision based on accuracy and complexity.
3) Fuzzification, implication using mamdani's operator and finally defuzzification to get desired output.

Fig. 2 shows the block diagram of the proposed FLC scheme. The designed rules for knowledge base are shown in Table 1. The top row and left column of the matrix indicate the fuzzy sets of the variables e and ce.

TABLE 1. FUZZY CONTROL RULE BASE

E / ce	NB	NM	NS	Z	PS	PM	PB
NB	NVB	NVB	NVB	NB	NM	NS	Z
NM	NVB	NVB	NB	NM	NS	Z	PS
NS	NVB	NB	NM	NS	Z	PS	PM
Z	NB	NM	NS	Z	PS	PM	PB
PS	NM	NS	Z	PS	PM	PB	PVB
PM	NS	Z	PS	PM	PB	PVB	PVB
PB	Z	PS	PM	PB	PVB	PVB	PVB

B. Proposed Fuzzy Logic Controller Interfacing

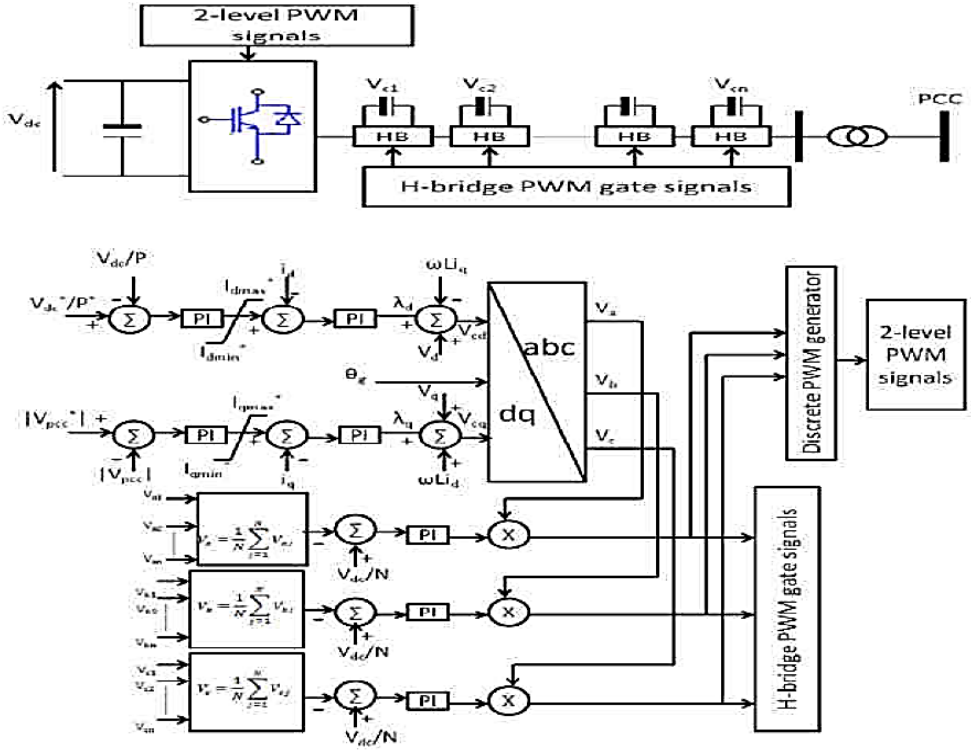

Fig. 4. Schematic diagram represents the control layer of the hybrid multilevel converter with ac side cascaded H-bridge cells

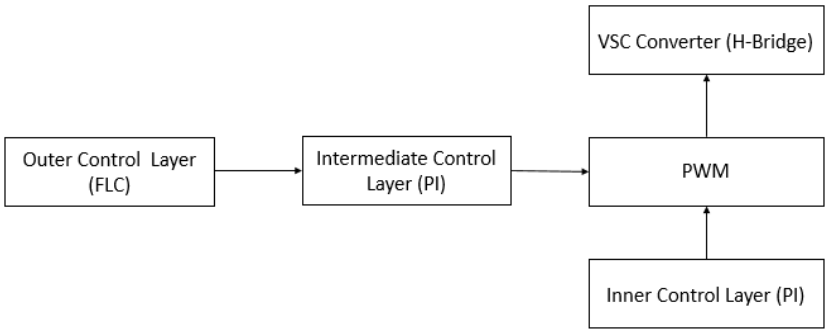

Fig. 5. Block diagram illustrating overview of the control scheme.

A HVDC transmission system based on a hybrid multilevel VSC with ac-side cascaded H-bridge cells requires three control system layers. The inner control layer represents the modulator and capacitor voltage-balancing mechanism that generates the gating signals for the converter switches and maintains voltage balance of the H-bridge cell capacitors. The intermediate control layer represents the current controller that regulates the active and reactive current components over the full operating range. The outer control layer is the dc voltage (or active power) and ac voltage (or reactive power) controller that provide set points to the current controllers. The current, power, and dc link voltage controller gains are selected using root locus analysis, based on the applicable transfer functions. Some of the controller gains obtained using root locus analysis give good performance in steady state but failed to provide acceptable network disturbance performance. Therefore, the simulation final gains used are adjusted in the time domain to provide satisfactory performance over a wide operating range, including ac and dc side faults. Fig. 4 summarizes the control layers of the hybrid multilevel VSC. Fig. 5 summarizes the control layers of the hybrid multilevel VSC. Here in this topology a control system is designed for DC voltage regulation by integrating fuzzy controller with a PI controller.

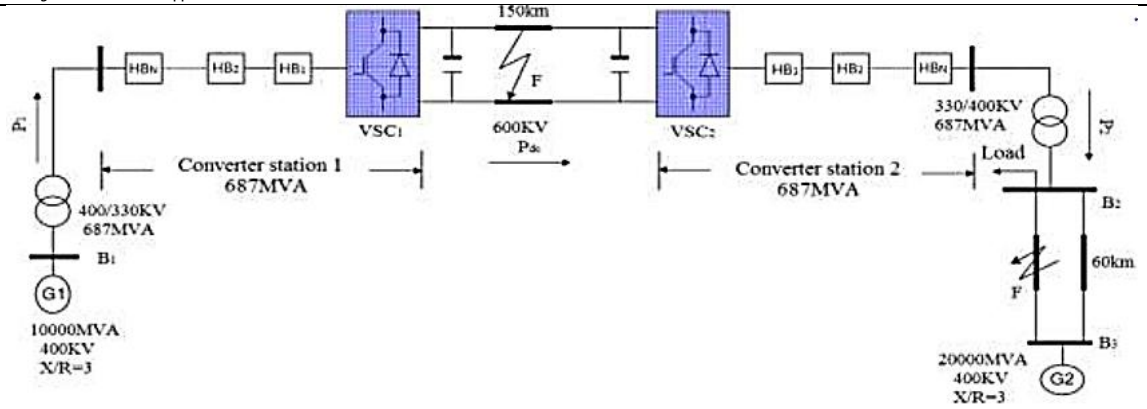

Fig. 6. Proposed HVDC transmission system

IV. SIMULATION RESULTS

The feasibility of the proposed system uses hybrid multilevel VSC with series H-bridges on ac side is explored, to importance the active show under any modification of the network. Under stable state the test network is shown in fig. 6. To explain the advantages of hybrid multilevel converters in case of ac and dc side faults. In the test network consists of three phases to ground fault on ac side in converter-2 with duration 140ms pole to pole dc fault on dc side with duration of 140ms.Each converter station having three phases and each phase connects with seven H-bridge cells in order to attain adequate simulation times without comparing outcome precision.

Hybrid multilevel converter with seven H-bridges per each phase to creates 29 voltage levels for each phase. Each H-bridge consists of 28 cells per arm with two switch modular multilevel converter having same voltage stresses and dc link voltage in both the converters. The converters are used to control active power, dc link voltage exchange and the results are seen in MATLAB Simulink model.

A. AC Network Faults

To demonstrate the ac fault ride-through capability of the presented HVDC system, the test network is subjected to a 140 ms three-phase fault to ground at the location shown in Fig. 6. During the fault period the power command to converter 1 is reduced in proportion to the reduction in the ac voltage magnitude. This is to minimize the two-level converter dc link voltage rise because of the trapped energy in the dc side, since power cannot be transferred as the voltage at B2 collapses. Fig. 7 displays the results when the test network exports 0.5 pu (343.5 MW) from grid G1to G2 and is subjected to the three-phase fault at t = 1s. Fig. 7(a) shows the active and reactive powers converter 1 exchanges with B1.Note that converter 1 matches its active power export to G2 in order to minimize the rise of converter 2 dc link voltage as its ability to inject active power into grid G2 reduces with the voltage collapse at B2, as shown in Fig. 7(d) and stated above. Fig. 7(b) shows the active and reactive powers that converter 2 injects into B2. The system is able to recover as soon as the fault is cleared, and converter 2 adjusts its reactive power exchange with grid G2 in order support voltage at B2. The transients shown of active and reactive powers at B2 are related to the reaction of the ac voltage controller that regulates the ac voltage at B2. Fig. 7(c) shows that the voltage magnitude at B2 remains unaffected; confirming that the hybrid voltage source multilevel converter does not compromise the HVDC transmission system's decoupling feature despite adopting active power matching at converter 1, as explained. Fig. 7(e) shows that converter 2 restrains its contribution to the fault current to less than full load current despite the voltage at B2 collapsing to 20% of its rated voltage, due to converter 2's current controller.

Fig. 7(f) shows that the H-bridge cell voltage stresses are controlled as the system rides through the ac-side fault. This confirms that the complexity of a HVDC system based on the hybrid multilevel VSC does not compromise its ac fault ride-through capability. Fig. 7(g) shows the hybrid multilevel VSC presents high-quality voltage to the converter transformer, with low harmonic content and dv/dt. This may permit elimination of ac-side filters and the use of standard insulation ac transmission transformers.

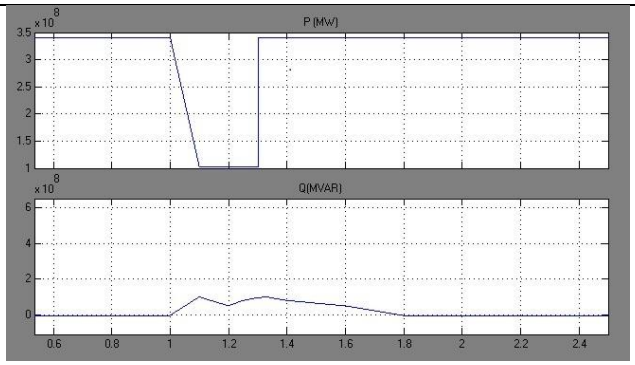

Fig. 7 (a)

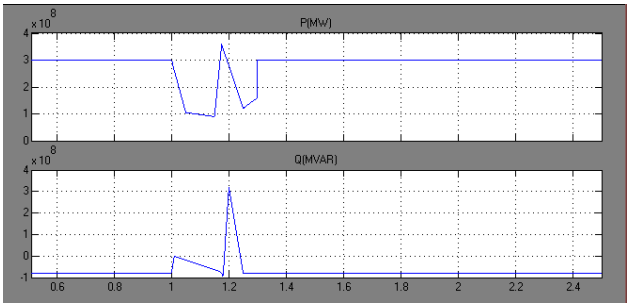

Fig. 7 (b)

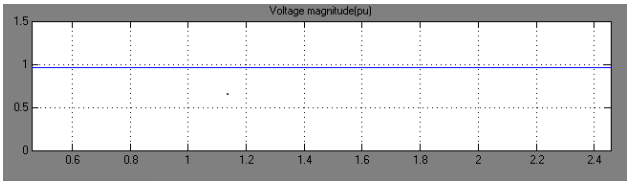

Fig. 7 (c)

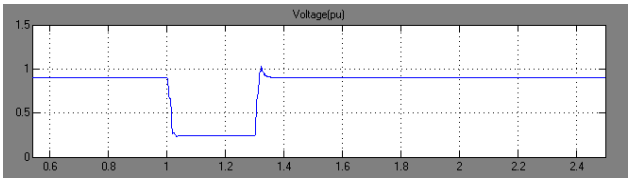

Fig. 7 (d)

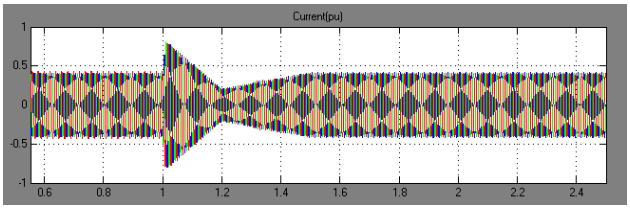

Fig. 7 (e)

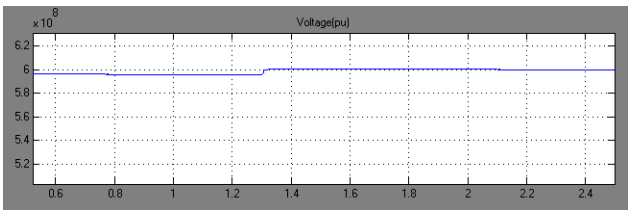

Fig. 7 (f)

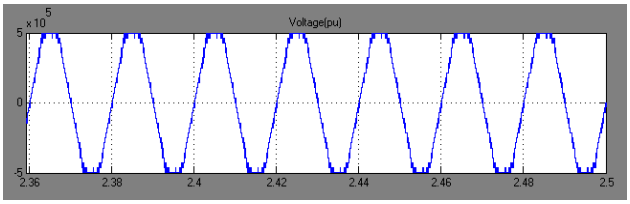

Fig. 7 (g)

Fig. 7. Waveforms demonstrating ac fault ride-through capability of HVDC transmission systems based on hybrid voltage multilevel converter with ac side cascaded H-bridge cells. (a) Active and reactive power converter 1 exchanges with B_1. (b) Active and reactive power converter 2 injects into B_2. (c) Voltage magnitude at B_1. (d) Voltage magnitude at B_2. (e) Current waveforms converter 2 injects into B_2. (f) Voltage across 21 H-bridge cells of the converter 2. (g) Line-to-line voltage waveform at the terminal of converter 1

B. DC Network Faults

The inherent current-limiting capability of the hybrid multilevel VSC with ac-side cascaded H-bridge cells that permits the VSC-HVDC system to ride-through dc-side faults will be demonstrated here. The test network is subjected to a 140 ms solid pole-to-pole dc-side fault at the location indicated in Fig. 6. During the dc-side fault period, active power exchange between the two grids G1 and G2 is reduced to zero. This facilitates uninterruptable system recovery from the temporary dc fault with minimal inrush current, since the power paths between the converter's ac and dc sides are blocked to eliminate a grid contribution to the dc fault.

Fig. 8 shows the results when the test network is subjected to a temporary solid pole-to-pole dc fault at the middle of the dc link. Fig. 8(a) and (b) shows the active and reactive powers that converter stations 1 and 2 exchange with B1 and B2. Observe zero active and reactive power exchange between the converter stations and ac grids G1 and G2 during the fault period, hence there is no current flow in the switches of converters 1 and 2. However, a large surge in active and reactive power is observed when the gating signals to converters 1 and 2 are restored after the fault is cleared, in order to restart the system. Fig. 8(c) shows that the current surge experienced by both converter stations causes noticeable voltage dipping at B1 due to increased consumption of reactive power during system start-up and dc link voltage build-up following fault clearance. The surge in active and reactive powers in both converter stations occurs as the dc side capacitors try to charge from both ac sides; this causes a large current flow from both ac sides to the dc side to charge the dc link capacitors and cable distributed capacitors as shown in Fig. 8(d) and 8(e). The results in Fig. 8(d) and 8(e) also demonstrate the benefits of dc fault reverse blocking capability inherent in this hybrid system, as the converter switches experience high current stresses only during dc link voltage build-up. Fig. 8(f) shows that converter 2 dc link voltage recovers to the pre-fault state after the fault is cleared. Notice the recovery period for the dc link voltage is relatively long; this is the major disadvantage of the proposed HVDC systems as it uses a common dc link capacitor. Fig. 8(g) expands the dc fault current and shows the 60-kA peak decays to zero in less than four cycles (for 50 Hz) after discharge of dc link and cable distributed capacitors. This result confirms the possibility of eliminating dc circuit breakers to isolate permanent dc side faults in dc networks that use HVDC converters with current limiting capability. Fig. 8(g) also shows the ac grids start to contribute to the dc link current after the fault is cleared, to charge the dc side capacitors. Fig. 8(h) shows the voltage across the 21 H-bridge cells of the converter stations 1 and 2.

The voltage across the H-bridge cell capacitors remains unaffected during the entire fault period as the converters are blocked. The cell capacitors start to contribute energy to the main dc link capacitors during dc link voltage build-up after restoration of the converter gating signals. This contribution creates a noticeable reduction in the cell capacitor voltages during system restart. The cell capacitors of converter 2 that regulate dc link voltage, experience a larger voltage dip than converter 1, which regulates active power. However, the reduction in H-bridge cell capacitor voltages is minimized if large capacitance is used.

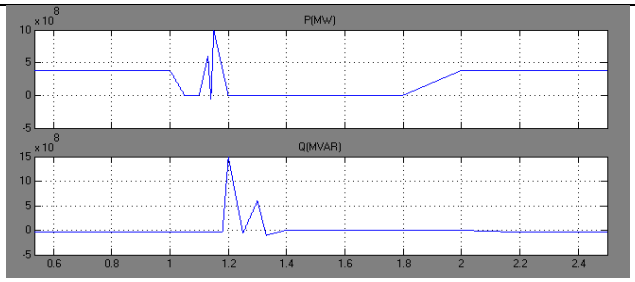

Fig. 8 (a)

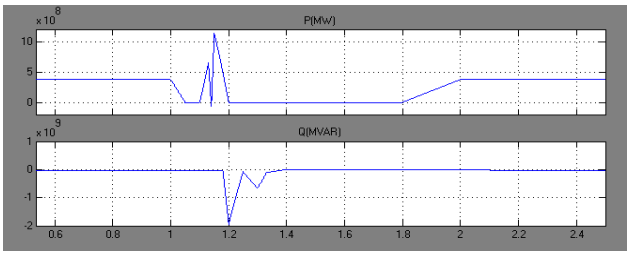

Fig. 8 (b)

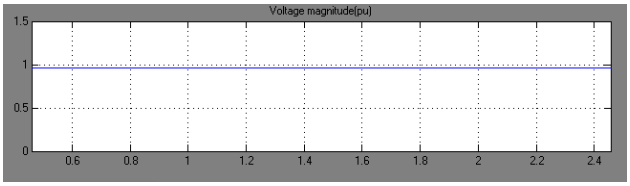

Fig. 8 (c)

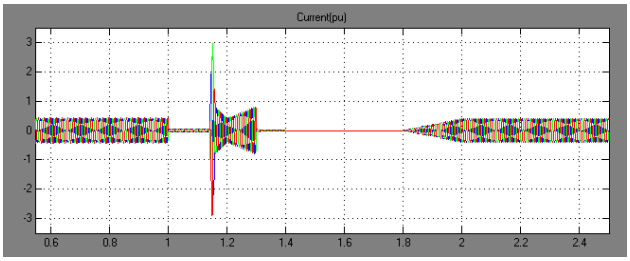

Fig. 8 (d)

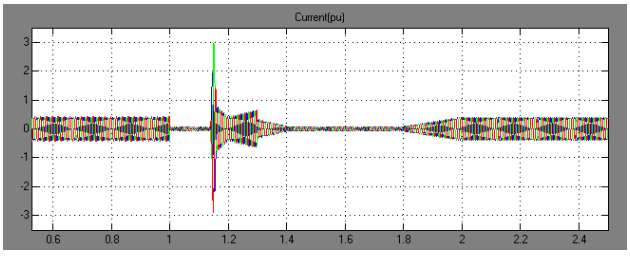

Fig. 8 (e)

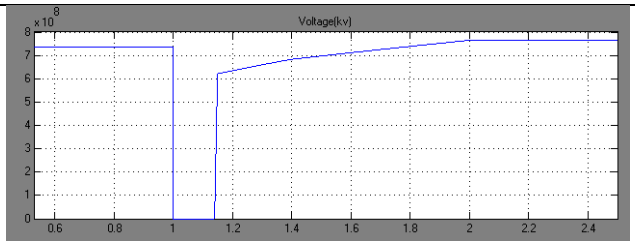

Fig. 8 (f)

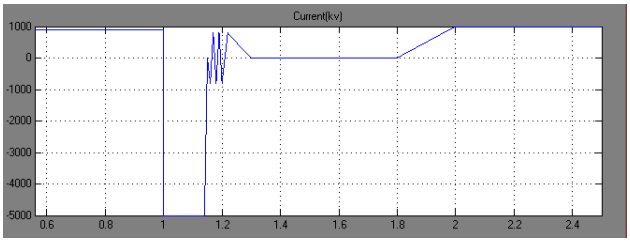

Fig. 8 (g)

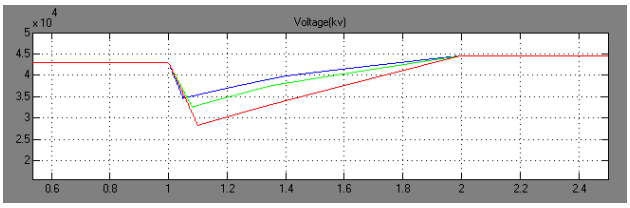

Fig. 8 (h)

Fig. 8. Waveforms demonstrating dc fault ride-through capability of HVDC transmission systems based on hybrid voltage multilevel converter with ac side cascaded H-bridge cells. (a) Active and reactive power converter 1 exchanges with B_1. (b) Active and reactive power converter 2 exchanges with B_2. (c) Voltage magnitude at B_1. (d) Current waveforms converter 1 exchange with grid at B_1. (e) Current waveforms converter 2 exchange with grid at B_2. (f) Converter 2 dc link voltage. (g) Zoomed version of dc link current demonstrating the benefits of dc fault reverse blocking capability. (h) Voltage across the H-bridge cell capacitors of converter 1.

V. CONCLUSION

This paper presented a new technique for minimization of ac and dc faults in voltage source control HVDC transmission system using Fuzzy Logic Controller (FLC). The proposed FLC hybrid multilevel converter an HVDC system is does not compromise the advantages of existing VSC-HVDC systems such as four-quadrant operation, black start capability and voltage support capability. In addition to existing VSC-HVDC system, proposed HVDC system provides inherent dc fault reverse blocking capability and resilient to ac side faults features. Voltage harmonics and current harmonics is reduced hence proposed HVDC system converter topology generate less harmonics, hence low filtering requirement on the ac sides and present high-quality voltage to the converter station transformer by generating higher pulse level. Potential small footprint and lower semiconductor losses compared to present HVDC systems.

REFERENCES

[1] G. P. Adam *et al.*, "Network fault tolerant voltage-source-converters for high-voltage applications," in *Proc. 9th IET Int. Conf. AC and DC Power Transmission*, London, U.K., 2010, pp. 1–5.

[2] Y. Zhang *et al.*, "Voltage source converter in high voltage applications: Multilevel versus two-level converters," in *Proc. 9th IET Int. Conf. AC and DC Power Transmission*, London, U.K., 2010, pp. 1–5.

[3] G. P. Adam *et al.*, "Modular multilevel inverter: Pulse width modulation and capacitor balancing technique," *IET Power Electron.*, vol. 3, pp. 702–715, 2010.

[4] M. M. C. Merlin *et al.*, "A new hybrid multi-level voltage-source converter with DC fault blocking capability," in *Proc. 9th IET Int. Conf. AC and DC Power Transmission*, London, U.K., 2010, pp. 1–5.

[5] Naumanen *et al.*, "Mitigation of high -originated motor over voltages in multilevel inverter drives," *IET Power Electron.,* vol. 3, pp. 681–689, 2010.

[6] Guanjun et al., "New technologies of voltage source converter (VSC) for HVDC transmission system based on VSC," in *Proc IEEE Power Energy Soc. Gen. Meeting—Conversion and Delivery of Electrical Energy in the 21st Century, 2008*, pp. 1–8.

[7] N. Flourentzou and V. G. Agelidis, "Optimizedmodulation for AC-DC harmonic immunity in VSC HVDC transmission," *IEEE Trans. Power Del.*, vol. 25, no. 3, pp. 1713–1720, Jul. 2010.

[8] Cuiqing et al., "Use of VSC-HVDC for industrial systems having onsite generation with frequency control," *IEEE Trans. Power Del., vol. 23, no. 4*, pp. 2233–2240, Oct. 2008.

[9] Z. Huang *et al.*, "Exploiting voltage support of voltage-source HVDC," *Proc. Inst. Electr. Eng.—Gen., Transm. Distrib.*, vol. 150, pp. 252–256, 2003.

[10] G. Kalcon *et al.*, "HVDC network: Wind power integration and creation of super grid," in *Proc. 10th Int. Conf. Environ. Electr. Eng.*, 2011, pp. 1–4.

[11] Hui et al., "Analysis of coupling effects on overhead VSC-HVDC transmission lines from AC lines with shared right of way," *IEEE Trans. Power Del., vol. 25*, pp. 2976–2986, 2010.

[12] B. T. Ooi and X. Wang, "Boost-type PWM HVDC transmission system," *IEEE Trans. Power Del.*, vol. 6, no. 4, pp. 1557–1563, Oct. 1991.

[13] P. Adam et al., "HVDC Network: DC fault ride-through improvement," *in Proc. Cigre Canada Conf. Power Syst., Halifax, NS,Canada, Sep. 6–8, 2011*, pp. 1–8.

[14] P. Adam et al., "Dynamic behaviour of five-level grid connected modular inverters*," in Proc. 9th Int. Conf. Environ. Electr. Eng., 2010*, pp. 461–464.

[15] M. Perez *et al.*, "Predictive control of AC-AC modular multilevel converters," *IEEE Trans. Ind. Electron.*, vol. 59, no. 7, pp. 2832–2839, Jul. 2012.

[16] L. A. Zadeh, "Fuzzy stes," Informat. Contr., vol. 8, pp. 338-353, 1965.

[17] P. Kirawanich and R. M. O. Connell, "Fuzzy logic control of an active power line conditioner*," IEEE Trans. on Power Electron., vol. 19, no. 6*, pp. 1574-1585, 2004.

[18] B. K. Bose, *Modern Power Electronics and AC drives*, Pearson Education Asia, 2002.

[19] R. C. Bansal, T. S. Bhatti and D. P. Kothari, "Artificial intelligence techniques for monitoring and control of power systems: an overview," *in Proc. Contr. Instrumentation Inform. Commun. Conf., Calcutta, India, 2001*, pp. 91–95.

[20] B. N. Singh, B. Singh, A. Chandra, P. Rastgoufard and K. Al-Hadded, "An improved control algorithm for active filters," *IEEE Trans. Power Delivery, vol. 22, no. 2*, pp. 1009-1020, Apr. 2007.

[21] N. Gupta, S. P. Dubey and S. P. Singh, "Neural network based shunt active filter with direct current control for power quality conditioning," *Int. J. Power Electron., in press.*

[22] W. Pedrycz, ''Why triangular membership functions,'' *Fuzzy Sets Syst., vol. 64*, pp. 21--30, 1994.

[23] A.I. Dounis and D.E. Manolakis, ''Design of a fuzzy system for living space thermal comfort regulation,'' *Appl. Energy, vol. 69, no. 1*, pp. 119-144, 2001.